



# APPLICATION OF ORTHOTROPIC CONSTITUTIVE MODEL INCORPORATED WITH SPH TO SIMULATE TENSILE FAILURE OF RC BEAM

Shahrul Niza Mokhatar<sup>1</sup>, Yoshimi Sonoda<sup>2</sup> and Jin Fukazawa<sup>2</sup>

<sup>1</sup>Jamilus Research Centre, Universiti Tun Hussein Onn Malaysia, Batu Pahat, Johor, Malaysia

<sup>2</sup>Structural Analysis Laboratory, Department of Civil Engineering, Kyushu University, Motooka, Fukuoka Japan

E-Mail: [shahruln@uthm.edu.my](mailto:shahruln@uthm.edu.my)

## ABSTRACT

The responses of reinforced concrete beams subject to low velocity impact loading are simulated using orthotropic constitutive model incorporated with Smoothed Particle Hydrodynamics (SPH) method. The tensile failure of the beam is using the orthotropic constitutive equation during the softening phase on tension region, where the three principle strain components for tension (positive value) and compression (negative value) are used independently. In order to validate the proposed model, two impact cases were analyzed. The first case is simulation of simply supported beam without shear rebar using SPH and FEM. The second case is involving the comparisons of impact case of RC beam using proposed model with existing experimental tests. By adopting orthotropic constitutive equation and tensile softening algorithm defined by damage parameter, flexural cracks and shear failure can be analyzed by tracing the local stress condition.

**Keywords:** orthotropic constitutive model, RC beam, impact loads.

## INTRODUCTION

A number of mathematical models dealing with the plastic constitutive law of concrete materials have been proposed by (Rabczuk *et al.* 2006), (Zhou *et al.* 2008) and (Park *et al.* 2005) subjected to various impact loads (such as collision and blast). However, the application of the precise constitutive model is very difficult due to their many material parameters. Then, by increasing the complexity of the model, the cost of the calculation can be also increased, and sometimes it is not useful for practical needs. In fact, the advanced existing plasticity model such as Bresler-Pister model, William-Warnke model, Ottosen model, Reimann model, or Hsieh-Ting-Chen model requires many parameter identification that corresponding to appropriate laboratory tests (tri-axial test, hydrostatic test, etc.). Thus, modification of one-parameter simple models (like Von Mises) are widely applied for practical use.

It has been recognized, many researchers such as (Unosson, 2009), (Kantar, 2011) and (Mokhatar, 2013) have successfully analyzed the elastic-plastic behaviour of RC elements under low velocity impact loads using a FEM. However, simulation of solid mechanics problem due to dynamic loads (impact, blast, etc.) can cause in the application of Finite Element Method (FEM) to many problems. Their difficulties and limitations have been discussed extensively among researchers. One of them is when the material deforms, the large relative movement of the connecting nodes cannot be tracked accurately if use a fixed mesh. Thus, the connectivity of arbitrarily distributed particles without using any mesh should be applied to provide stable numerical solutions. Smoothed Particle Hydrodynamics (SPH) can be a superior to the FEM to solve the limitation in the mesh based technique. The SPH technique does not require a pre-defined mesh to render any connective of the particles during the process

of computation. Besides, the SPH particles also carry material properties, and are allowed to move in light of the internal interactions and external forces. During recent years, the application of mesh-less methods has been widely used for the high-velocity impact (HVI) computation to the problems of solid mechanics. Further, (Swaddiwudhipong *et al.* 2010) and (Johnson, 2011) have been successfully applied SPH to study the perforation/penetration of steel and plain concrete subjected to HVI loads. However, in the present study, the responses of simply reinforced concrete beams subjected to low velocity impact loading are numerically analyzed. The analysis is performed using orthotropic constitutive model incorporated with SPH.

In this study, the constitutive model plays an important role to simulate the material behaviour. Most constitutive models are based on the theories of elasticity and plasticity. The linear elastic model based on the generalized Hooke's law is still widely adopted for the elastic materials by far for its simplicity. When the Continuous, Homogenous, Isotropic and Linear Elastic is adopted, the model can be determined by the Young's modulus ( $E$ ) and the Poisson's ratio ( $\nu$ ). Based on that, more sophisticated models for isotropic condition can also be easily derived. To simulate the strength of materials in various states, failure criteria defined with stress invariants were developed based on 1-parameter criterion. Many researchers such as (Bresler *et al.* 1958), (William *et al.* 1975), (Ottosen, 1977) or (Hsieh *et al.* 1982) have attempted to extend the application of plasticity model until 3- to 5-parameter criterion. However, this study considered 1-parameter criterion to describe deformational characteristics of materials in the ultimate stress state.



## CONSTITUTIVE MODEL

Elastic-plastic constitutive equation of pressure independent (von Mises criteria)

When the second invariant of deviatoric stress tensor,  $J_{2D}$  reaches a certain value, yielding or plastic domain will take place. Von Mises (VM) in a year 1913 called this criterion as distortional energy theory or shearing-stress criteria. In which when distortional energy reaches a value that is equal to the distortional energy at yield in simple tension, the yielding is occurred. The VM yield surfaces in principal stress coordinate circumscribes a cylinder with radius  $\sqrt{2/3}\sigma_y$  around the hydrostatic axis as shown in the Figure-1. By this criterion, the effect of hydrostatic pressure on compression domain is neglected. This phenomenon is quite reasonable for metal plasticity. In this paper, some example will be presented by employing this yield criterion with modification to simulate the impact response of RC beam.

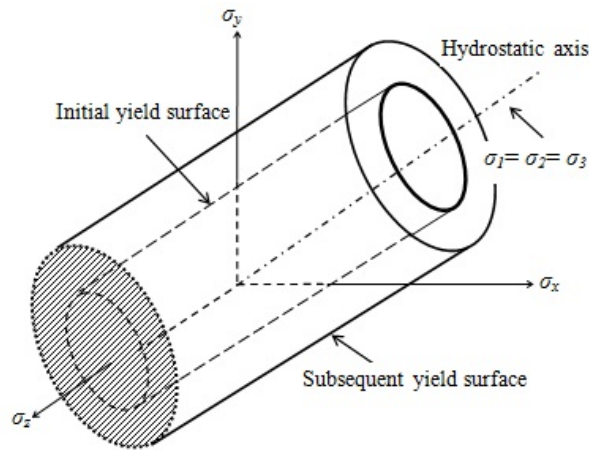


**Figure-1.** Graphic representation of VM with hardening criteria.

\*  $\sigma_{x,y,z}$  &  $\sigma_{1,2,3}$  = stress corresponds to x, y, z-axis.

$$[D]^p = \frac{9\mu^2}{\sigma_{eqs}^2(H'+3\mu)} \begin{bmatrix} \sigma_{11}^2 & \sigma_{11}^2 \sigma_{22}^2 & \sigma_{11}^2 \sigma_{33}^2 & \sigma_{11}^2 \sigma_{12}^2 & \sigma_{11}^2 \sigma_{23}^2 & \sigma_{11}^2 \sigma_{31}^2 \\ & \sigma_{22}^2 & \sigma_{22}^2 \sigma_{33}^2 & \sigma_{22}^2 \sigma_{12}^2 & \sigma_{22}^2 \sigma_{23}^2 & \sigma_{22}^2 \sigma_{31}^2 \\ & & \sigma_{33}^2 & \sigma_{33}^2 \sigma_{12}^2 & \sigma_{33}^2 \sigma_{23}^2 & \sigma_{33}^2 \sigma_{31}^2 \\ & & & \sigma_{12}^2 & \sigma_{12}^2 \sigma_{23}^2 & \sigma_{12}^2 \sigma_{31}^2 \\ & & & & \sigma_{23}^2 & \sigma_{23}^2 \sigma_{31}^2 \\ & & & & & \sigma_{31}^2 \end{bmatrix} \quad (5)$$

## Tensile Softening – Elastic Degradation

The flexural/bending cracking is common prominent features on concrete failure mode occurred in the tension zone. It has been known that this tensile cracking degrades the stiffness of concrete material. Thus, this paper considers the local material orthotropy caused by tensile failure of concrete, in which the failure initiates the decrease of elastic stiffness normal to the crack

According to this criterion, the function of the VM,  $f_{VM}$  model can be expressed by,

$$f_{VM}(J_{2D}) = J_{2D} - k^2 < 0 \quad \therefore \text{elastic} \quad (1a)$$

$$f_{VM}(J_{2D}) = J_{2D} - k^2 = 0 \quad \therefore \text{plastic} \quad (1b)$$

where  $k$  is the material constant and the second invariant of deviatoric stress,  $J_{2D}$  consists of stress tensor,  $\sigma_{ij}$  can be derived as below;

$$J_{2D} = \frac{1}{2} \sigma'_{ij} \sigma'_{ij} \quad (2)$$

and the deviatoric stress  $\sigma'_{ij}$ , can be written as

$$\sigma'_{ij} = \sigma_{ij} - \frac{1}{3} \sigma_{mm} \delta_{ij} \quad (3)$$

Finally, the incremental of stress,  $d\sigma_{ij}$  for VM that used in this study can be simplified as below

$$d\sigma_{ij} = \left[ D_{ijkl}^e - \frac{4\mu^2 \sigma'_{ij} \mu \sigma'_{kl}}{\frac{4}{9} H' \sigma_{eqs}^2 + 2\mu \sigma'_{ab} \sigma'_{ab}} \right] \delta_{ik} \delta_{jl} d\epsilon_{kl} \\ = \left[ D_{ijkl}^e - \frac{\mu^2 \sigma'_{ij} \sigma'_{kl}}{\frac{1}{9} H' \sigma_{eqs}^2 + \mu \frac{1}{3} \sigma_{eqs}^2} \right] \delta_{ik} \delta_{jl} d\epsilon_{kl} \quad (4)$$

and the matrix form of  $[D]^p$  can be formed by equation (5).

direction. The plasticity and damage are directly defined after exceeding the tensile strength,  $\sigma_t$  using the linear softening path. The stiffness degradation of the concrete materials in tensile side can be identified by linear tension-softening path as shown in Figure-2. In addition, the ultimate strain  $\epsilon_{cre}$  (end point of softening path) is assumed and its adequate value is chosen in order to prevent



particle size dependency using the relation between fracture energy  $G_f$  and particle size,  $d^0$ .

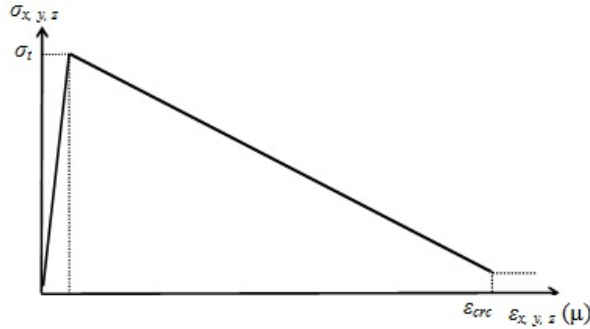


Figure-2. Linear strain-softening.

A cracking of the material is assumed to arise in the direction normal to the principal tensile strain. The integrity tensor  $\varphi_i^+$  ( $i = x, y, z$ ) is introduced only in a tensile

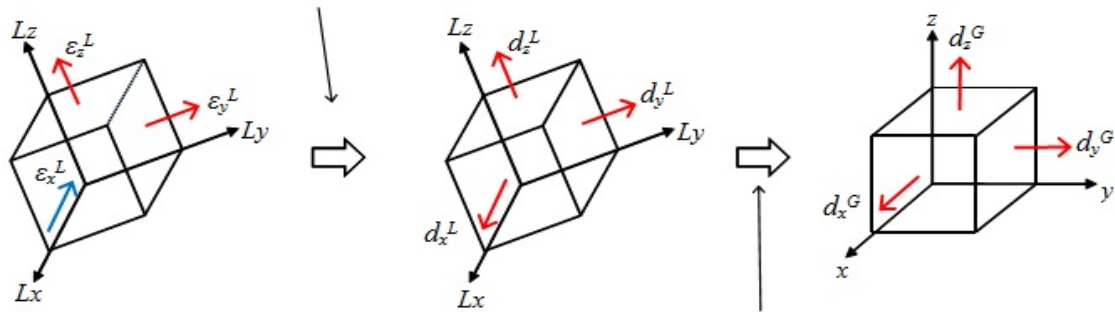
side by considering the positive values of principal strain. Figure-3 shows the chronology of calculation for integrity tensor. In which the principal value and its direction are calculated by eigenvalue analysis based on each of the strain components on target particle. Then, the damage parameter  $d_x^L, d_y^L, d_z^L$  (in the local coordinate) are calculated by using the calculated principal positive values as shown in equation (6a-6c).

$$d_x^L = \frac{\varepsilon_x^+}{\varepsilon_{crc}} \quad (6a)$$

$$d_y^L = \frac{\varepsilon_y^+}{\varepsilon_{crc}} \quad (6b)$$

$$d_z^L = \frac{\varepsilon_z^+}{\varepsilon_{crc}} \quad (6c)$$

Extracted positive value of the principal strain of the tensile component to calculate the damage parameter



Calculates the degree of damage in the global coordinate system

Figure-3. Chronology of calculation for damage parameter.

Finally, transform the damage parameter in the local coordinate to the global coordinate in order to calculate the integrity tensor  $\varphi_x, \varphi_y, \varphi_z$ .

$$(\varphi_x^+)^2 = 1 - d_x^G \quad (7a)$$

$$(\varphi_y^+)^2 = 1 - d_y^G \quad (7b)$$

$$(\varphi_z^+)^2 = 1 - d_z^G \quad (7c)$$

Then, the damage formulations according to equation (7) are multiplied to the initial fourth-order

isotropic elastic matrix to form the orthotropic constitutive equation.

$$\sigma_{ij} = \varphi_x^+ \varphi_y^+ \varphi_z^+ [D_{ijkl}^e] \varepsilon_{kl} \quad (8)$$

Finally, their stiffness matrix can be formed as shown in equation (9).

$$[D]^* = \begin{bmatrix} \varphi_x^2(\lambda+2\mu) & \varphi_x\varphi_y\lambda & \varphi_x\varphi_z\lambda & 0 & 0 & 0 \\ \varphi_y^2(\lambda+2\mu) & \varphi_y\varphi_x\lambda & \varphi_y\varphi_z\lambda & 0 & 0 & 0 \\ \varphi_z^2(\lambda+2\mu) & \varphi_z\varphi_x\lambda & \varphi_z\varphi_y\lambda & 0 & 0 & 0 \\ \varphi_x\varphi_y2\mu & \varphi_y\varphi_x2\mu & 0 & 0 & 0 & 0 \\ \varphi_x\varphi_z2\mu & 0 & \varphi_z\varphi_x2\mu & 0 & 0 & 0 \\ \varphi_y\varphi_z2\mu & 0 & 0 & \varphi_z\varphi_y2\mu & 0 & 0 \end{bmatrix} \quad (9)$$



## NUMERICAL EXAMPLES

### Envelope of VM Models and its Stress Strain Curve

The tensile strength of concrete/mortar materials is much lower than the compression strength; hence, in many cases, material failure is mainly caused by tensile failure. In this analysis, the elastic-plastic constitutive equation of pressure independent (VM criteria) is assumed for both material concrete and steel reinforcement. Then, the linear softening path is utilized to degrade the tensile stiffness. The envelope of the VM model associated with tensile cut-off is shown in Figure-4 for concrete materials

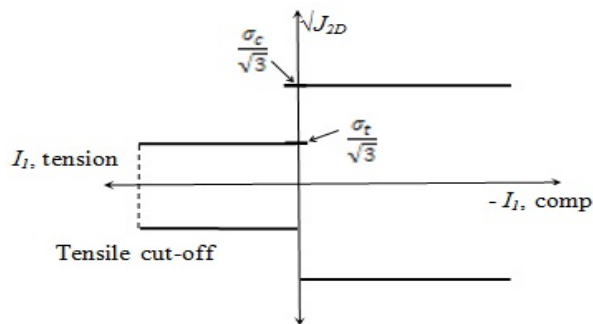


Figure-4. Envelope for VM models.

Meanwhile, the stress-strain curve represents the behaviour of both materials can be obtained in Figure-5 (a)-(b).

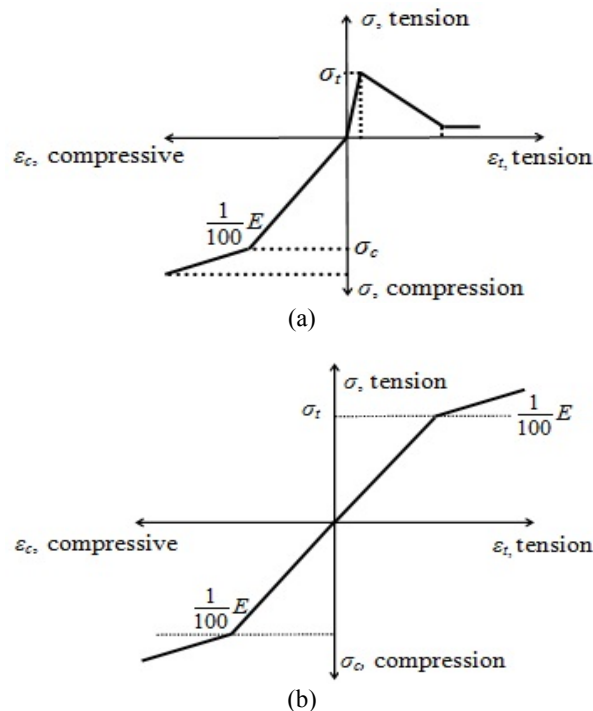


Figure-5. Stress-strain curve presents the behavior of both materials.

### Comparisons of Impact Case of Simply Supported Beam without Shear Rebar using SPH and FEM

The numerical analysis of SPH and FE was conducted by applying simply supported beam [see Figure-6] reinforcing by two main rebar in the bottom region. The objective of this analysis is to investigate an ability of a proposed numerical scheme incorporated with pressure independent criterion for calculating the displacement-time response of the RC beam subjected to low velocity impact loading using SPH method.

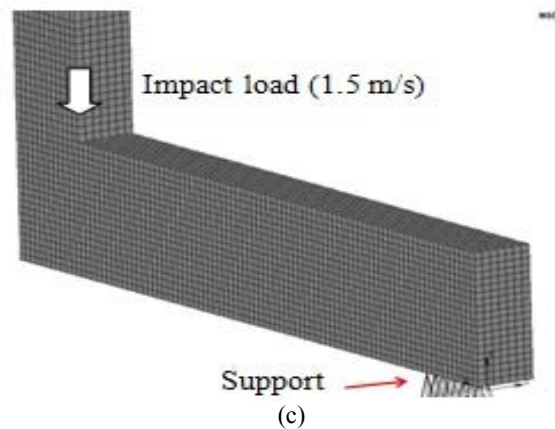
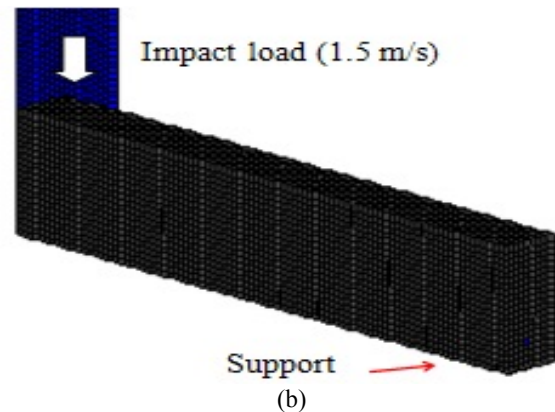
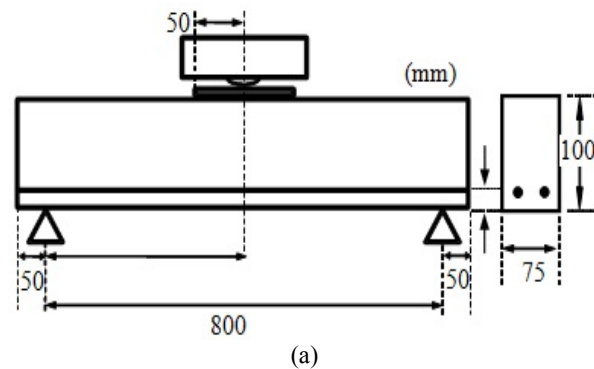


Figure-6. (a) Beam details and (b) (c) its analytical quarter model.



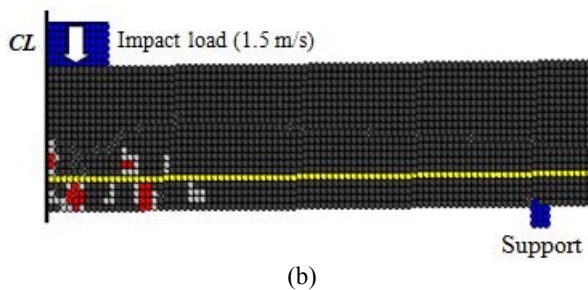
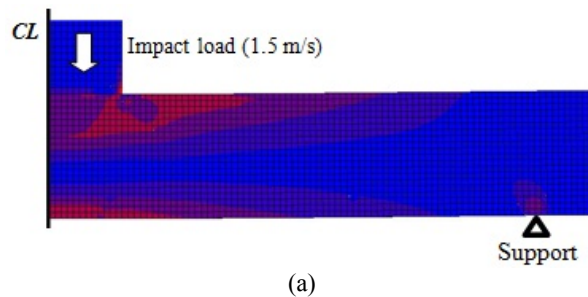


Table-1 shows the material properties of concrete and steel reinforcement in which the size of the particle and the element for both numerical methods is 0.005 m. In this analysis, low velocity impact load of 1.5 m/s is imposed onto the beam in order to compare the displacement response between SPH and FEM.

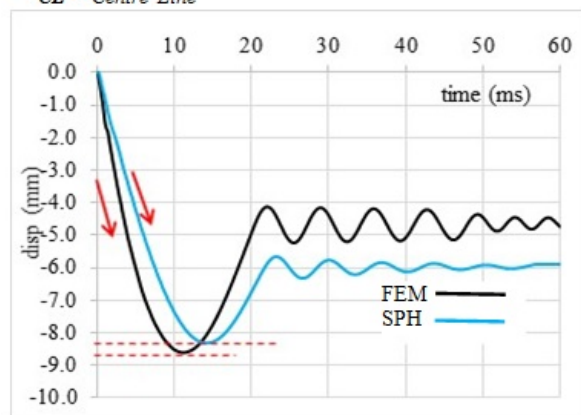
**Table-1.** Material properties.

Material	$E$ N/m <sup>2</sup>	$\nu$	$\rho$ kg/m <sup>3</sup>	$\sigma_t$ N/m <sup>2</sup>	$\sigma_c$ N/m <sup>2</sup>
Mortar	$11900 \times 10^6$	0.3	2350	$1.7 \times 10^6$	$17 \times 10^6$
Steel	$210000 \times 10^6$	0.22	7850	$300 \times 10^6$	$300 \times 10^6$

\*Yield stress in compression =  $\sigma_c$  Young Modulus =  $E$   
Yield stress in tension =  $\sigma_t$ , Density =  $\rho$ , Poisson's ratio =  $\nu$



\* CL = Centre Line



(c)

**Figure-7.** Results for both FEM and SPH methods.

Since the objective of this numerical example to compare the displacement response between SPH and FEM, the crack pattern and overall impact response in Figure-7 (a) and (b) are not discussed in details. Based on Figure-7 (c), it can be seen that the FEM and SPH analysis showed a close peak displacement of approximately 8.6 mm and 8.4 mm, respectively. The FEM curves seem to dampen out earlier compared to SPH. In addition, there is also some difference in the shape of displacement curve and periods of vibrations. This might be due to the parameter value used for the softening technique and affected by the existing concrete material model in the FEM commercial software. Proper determination of the time step is also necessary to produce well-agreed curve for both analyses.

Based on the close peak displacement value showed by both analyses, it can be concluded that SPH methods associated with the derived modified VM yield criteria are able to produce a similar displacement response with FEM. However, further validation with the experimental results is required to investigate the ability of the SPH method accompanied with modified VM criterion and softening technique.

#### Comparisons of Impact Case of RC Beam using Proposed Model with Existing Experimental Tests

The nonexistence of the mesh elements in SPH method and the independent calculation of relations among the particles results/beget to paramount ways in the bending deformation and cracking analysis of RC structures. Therefore, an attempt has been made in the second example to examine the accuracy and ability of the SPH method by utilizing softening technique, with regards to assessing the response of RC elements (beam) due to impact forces in term of shear cracking and bending failure. The numerical capabilities were extensively verified against existing experimental result by (Chen *et al.* 2009). The beam details are shown in Figure-8.

Practical test was carried out by literatures investigating high mass – low velocities (5.3 m/s) impact behavior of reinforced concrete beam and resulting dynamic response of the total structure. The total size of the beam is 200 mm x 100 mm in depth and width, while, 3000 mm (2700 mm span) in length. The beam is reinforced with 6 mm diameter and 12 mm diameter high yield steel bars as top and bottom reinforcement respectively. The concrete cover between the main reinforcement bars and the top and bottom edges of the beam is 20 mm. The stirrups of 6 mm are spaced at 200 mm intervals. In addition, a flat impact mass is used. The diameter of it is 100 mm, and the weight of it is 98.7 kg. The numerical simulations of the beam exploit the symmetric model to simplify the analysis and were supported 150 mm from the ends. The steel and concrete properties employed in this model are shown in Table-2.

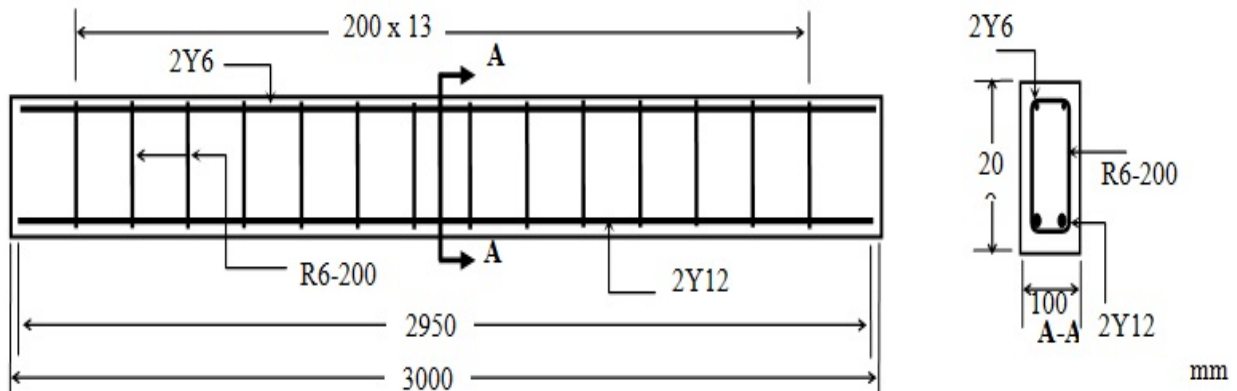


Figure-8. Beam details.

Table-2. Material properties.

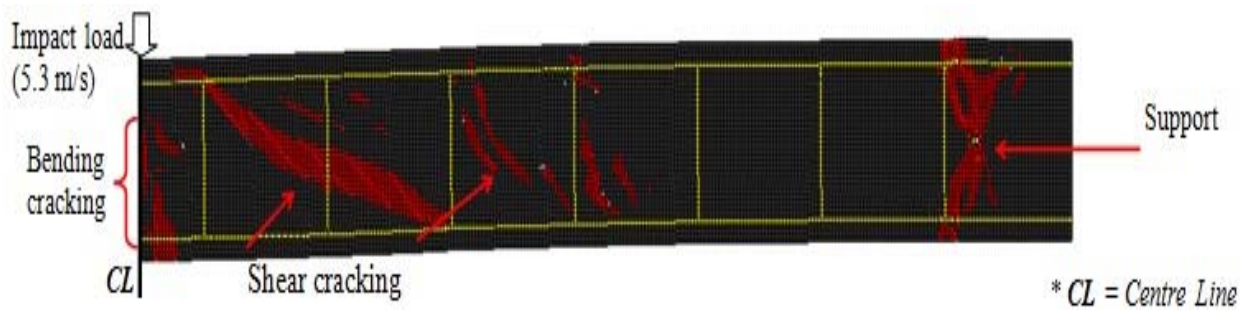
Material	$E$ N/m <sup>2</sup>	$\nu$	$\rho$ kg/m <sup>3</sup>	$\sigma_c$ N/m <sup>2</sup>	$\sigma_t$ N/m <sup>2</sup>
Concrete	$20600 \times 10^6$	0.22	2400	$45 \times 10^6$	$4.5 \times 10^6$
Steel	$206000 \times 10^6$	0.3	7800	$300 \times 10^6$	$300 \times 10^6$

\*Yield stress in compression =  $\sigma_c$ , Young Modulus =  $E$

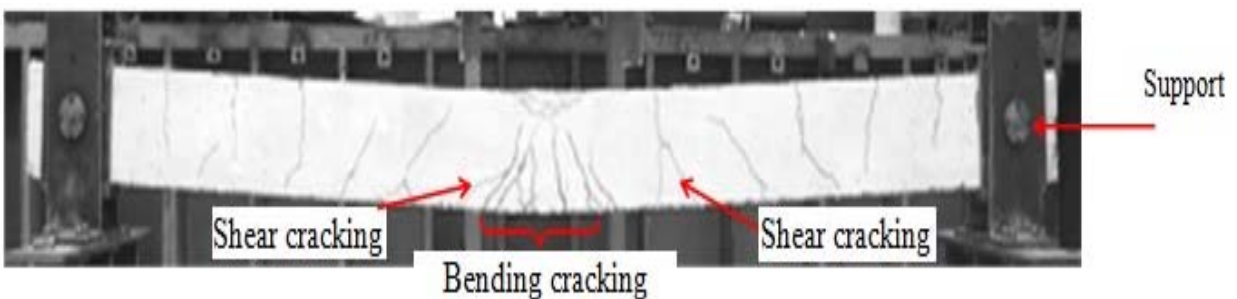
Yield stress in tension =  $\sigma_t$ , Density =  $\rho$ , Poisson's ratio =  $\nu$

experimental investigations by (Chen *et al.* 2009). The proposed model presents comparable results in term of propagations of vertical cracking, bending cracking and inclined cracking tendency. In addition, the calculation of maximum displacement of the 2700 mm span beam and its displacement curve are accurately analyzed as shown in Figure-9 (c). This figure also verified that the bending behaviour is well correspond to the experimental results. However, some differences in the oscillation periods are investigated. This phenomenon could be improved by modifying the artificial viscosity parameter and other constant value used in this calculation.

According to the Figure-9 (a), the result from numerical simulations shows good agreement with



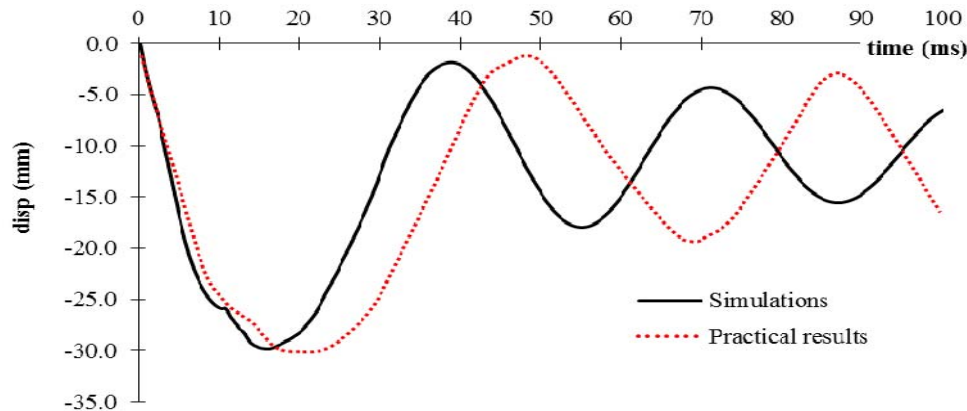
(a) Simulation results (quarter model)



(b) Experimental results



www.arpnjournals.com



(c) Displacement – time histories

**Figure-9.** Results for both numerical and experimental tests.

## CONCLUSIONS

This paper precisely explains about the orthotropic constitutive equation and presented some numerical example of the impact analysis on the RC beam. The comparison between SPH and FEM as well as simulation and experimental tests were determined the ability of the proposed numerical method when simulating RC beam subjected to low velocity impact load. By adopting orthotropic constitutive equation and tensile softening algorithm defined by damage parameter, flexural cracks and shear failure can be analyzed by tracing the local stress condition.

However, this analysis only treats pressure independent criterion for concrete materials by ignoring the effect of confining pressure in the compression zone. According to the characteristics of concrete and the high-pressure range of an impact phenomenon on this material, the pressure dependent criterion is significantly important to evaluate accurate material strength and their inelastic failure behaviour of concrete/mortar under compression forces. A pressure dependent model is required when simulating cementitious (concrete/mortar) materials because of this model considering confined pressure in the highly compressible conditions.

## REFERENCES

- [1] Bresler, B. and Pister, K. S. (1958). Strength of Concrete under Combined Stresses. American Concrete Institute, 55(9), pp. 321--345.
- [2] Chen, Y. and May, I. M. (2009). Reinforced concrete members under drop-weight impacts, Proceedings of the Institution of Civil Engineers, 162(1): pp. 45-56.
- [3] Fukazawa, J. and Sonoda, Y. (2011). An accuracy of impact failure response of reinforced concrete beam using ASPH method. Journal of Structural Engineering, Japan Society of Civil, 57A, pp. 1205--1212. (Japanese).
- [4] Hsieh, S. S., Ting, E. C. and Chen, W. F. (1982). A Plastic-Fracture Model for Concrete. International Journal of Solids and Structures, 18(3), pp. 181--197.
- [5] Johnson, G. R. (2011). Numerical algorithms and material models for high-velocity impact computations. International Journal of Impact Engineering, 38(6), pp. 456--472.
- [6] Kantar, E., Erdem, R. T. and Anil, O. (2011). Nonlinear finite element analysis of impact behavior of concrete beam. Mathematical and Computational Applications, (1), pp. 183--193.
- [7] Mokhtar, S. N., Abdullah, R. and Kueh, A. B. H. (2013). Computational impact responses of reinforced concrete slabs. Computers and Concrete, An International Journal, 12(1), pp. 37--51.
- [8] Ottosen, N. S. (1977). A Failure Criterion for Concrete. Journal of the Engineering Mechanics Division, 103(4), pp. 527--535.
- [9] Park, H. and Kim, J. Y. (2005). Plasticity model using multiple failure criteria for concrete in compression. International Journal of Solids and Structures, 42(8), pp. 2302--2322.
- [10] Rabczuk, T. and Eibl, J. (2006). Modelling dynamic failure of concrete with meshfree methods. International Journal of Impact Engineering, 32(11), pp. 1878--1897.
- [11] Swaddiwudhipong, S., Islam, M. J. and Liu, Z. S. (2010). High velocity penetration/perforation using coupled smoothed particle hydrodynamics-finite element method. International Journal of Protective Structures, 1(4), pp. 489--506.
- [12] Tokumaru, S., Sonoda, Y., Fukazawa, J. and Shahrul Niza Mokhtar. (2011). A fundamental study on the



impact failure mechanism of reinforced mortar beam using SPH method. Proceeding of the Japan Concrete Institute, 33, pp. 775--780. (Japanese).

- [13] Unosson, M. (2009). Numerical simulations of the response of reinforced concrete beams subjected to heavy drop tests, Fourth International Symposium on Impact Engineering, 1, pp. 613--618.
- [14] William, K. J. and Warnke, E. P. (1975). Constitutive Models for the Triaxial Behavior of Concrete, Proceedings of the International Assoc. for Bridge and Structural Engineering, 19, pp. 1--30.
- [15] Zhou, X. Q., Kuznetsov, V.A., Hao, H. and Waschl, J. (2008). Numerical prediction of concrete slab response to blast loading. International Journal of Impact Engineering, 35(10), pp. 1186--1200.